Proton-stopping power of argon, krypton, and xenon

E. J. McGuire
Sandia National Laboratories, Division 1231, P.O. Box 5800, Albuquerque, New Mexico 87185
(Received 1 December 1982)

Parameters for the Bethe stopping-power theory for Ar, Kr, and Xe are obtained both via integration over optical oscillator strengths and from explicit plane-wave Born-approximation calculations. The former procedure produces a Bethe mean excitation energy (I) significantly lower than that measured, while the latter procedure produces I values within 10 eV of the measured values for Ar and Kr. For Xe the experimental I value lies midway between the two calculated I values. Inner-shell corrections are obtained from the explicit calculations. The K-shell corrections (C_K) are a factor of 2 larger than those obtained from hydrogenic calculations. The total inner-shell correction ($\sum_{nl} C_{nl}$) is in qualitative agreement for Ar, Kr, and Xe with results from a statistical model. However, the quantitative difference between the two sets of inner-shell corrections leads to significant increases in I values inferred from experimental measurements below 1 MeV proton energy.

I. INTRODUCTION

The extraction of a Bethe[1] mean excitation energy (I) from experimental proton stopping power data is a complex task.[2] In the Bethe[1] formula the nonrelativistic stopping power is proportional to

$$\ln(4M_eE_p/M_pI)=\ln(4mME_p/M_p)-\ln I \ , \qquad (1)$$

where M_e and M_p are the electron and proton masses, E_p is the proton energy, and I is the Bethe mean excitation energy. Since the Bethe theory is correct asymptotically as E_p goes to infinity, measurements at large E_p are suggested. Unfortunately, at large E_p the $\ln E_p$ term dominates the $\ln I$ term so such measurements require great precision. Further, since the variation in stopping power due to variation in I is small, other small effects (relativity, Z_1^3, and Z_1^4 corrections, and inner-shell corrections) must be included in the data analysis. This paper addresses, among other issues, the question of inner-shell corrections in Ar, Kr, and Xe.

Recently we carried out calculations on the proton-stopping power of Al (Ref. 3) and Au (Ref. 4) ions. The calculations were done in the plane-wave Born approximation (PWBA); that is, generalized oscillator strengths (GOS) for ionization and excitation of each occupied subshell were calculated. From these the subshell stopping power was obtained, and a sum over subshells produced the total stopping power. For the contribution of excitation to stopping power, the final-state sum was truncated. For example, for Ar the sum over excited levels was limited to levels with principal quantum numbers $n=4$—6, with n values increased by 1 for Kr and by 2 for Xe. Higher-lying levels were not included in either the GOS calculations, or the optical oscillator strength. For the ionization GOS, explicit calculations were limited to continuum electron energy $\mathscr{E} \lesssim 50\ E_{nl}$, where E_{nl} is the ionization energy of the nl subshell. For $\mathscr{E} \gtrsim 50\ E_{nl}$ the subshell GOS was approximated by $N_{nl}\delta(\mathscr{E}-K^2)$, where N_{nl} is the number of electrons in the nl subshell and K^2 is the momentum transfer. Since the summed subshell optical oscillator strength Z_{nl} is, in general, not equal to N_{nl}, the subshell GOS summed over energy at fixed momentum transfer is not a constant but is a function of momentum transfer. Physical reasons for the choice N_{nl} as the coefficient of the δ function, and consequences thereof, are discussed elsewhere.[5]

In addition to calculations of GOS on the Al and Au ions, extensive but not exhaustive calculations were done for neutral atoms. For Ar, Kr, and Xe the calculations were exhaustive and these elements are studied here. In Sec. II, Ar, Kr, and Xe stopping powers, calculated explicitly, are compared with experiment, and results obtained from the optical oscillator strengths are compared with other calculations. In Sec. III comparable results are obtained on a subshell basis from the explicit calculations and compared with those obtained from the calculations using optical oscillator strengths. In Sec. IV, innershell corrections are obtained and compared with other calculations. The Z^3 and Z^4 corrections are discussed in Sec. V, and the conclusions are in Sec. VI.

II. TOTAL STOPPING POWER

The calculated Ar, Kr, and Xe proton stopping powers between 0.1 and 10 MeV are shown in Fig. 1 as solid lines. The experimental data of Reynolds *et al.*,[6] Chilton *et al.*,[7] Swint *et al.*,[8] and Brolley and Ribe[9] are shown as squares, circles, triangles and diamonds, respectively. For Kr above 0.1 MeV and Ar above 0.4 MeV, the calculations and experimental data agree to better than 10 percent. For Xe the calculations are lower than the measurements of Ref. 6, higher than the measurements of Ref. 7, and in reasonable agreement with the measurement of Ref. 9. In general, the calculations are lower than the measurements. Since the Bethe formula contains the term $\ln(4M_eE_p/M_pI)$, the explicit calculations being lower than the data, suggests that the calculated I value will be larger than that extracted from experiment.

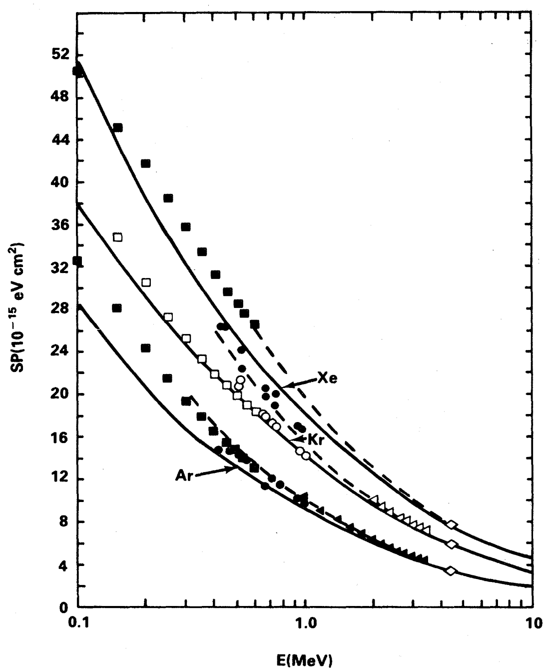

FIG. 1. Total stopping power of Ar, Kr, and Xe calculated in the plane-wave Born approximation (solid lines) and the measured values of Refs. 6–9, squares, circles, triangles and diamonds, respectively. The solid (open) points are for Ar and Xe (Kr). The dashed lines are the sum of calculated stopping power and empirical Z^3 and Z^4 corrections, as discussed in Sec. V.

The I values were evaluated via the optical oscillator strengths, i.e.,

$$Z_e \equiv \sum_{n,l} Z_{nl} = \sum_{n,l;n',l'} f_{nl,n'l'}(0) \;, \tag{2}$$

$$Z_e \ln I \equiv \sum_{n,l} Z_{nl} \ln I_{nl} = \sum_{n,l;n',l'} f_{nl,n'l'}(0) \ln(E_{nl} - E_{n'l'}) \;. \tag{3}$$

I also use the notation

$$Z_e \ln I = L(0) = \sum_{n,l} L_{nl}(0) = \sum_{n,l} Z_{nl} \ln I_{nl} \;. \tag{4}$$

In Table I are shown the Z_e, $L(0)$, and I values for Ar, Kr, and Xe, the Ar values of Dehmer *et al.*,[10] and the experimental I values of Ref. 2. For Ar the I value is in reasonable agreement with the calculation of Ref. 10, but significantly lower (10%) than the experimental value. For Kr the I value, calculated from the optical oscillator strengths, is 12% lower than the experimental value, while the Xe value is 9% lower. As mentioned above, comparing the explicit Born-approximation calculations with experiment suggested that the calculated I value would be too large. The I values of Ref. 2 are obtained after correction for target Z^3 and Z^4 effects. The explicit calculations do not include Z^3 and Z^4 effects. Thus, the I values are compared on the same basis. The Z^3 and Z^4 corrections are relevant to Fig. 1 and are discussed in Sec. V.

TABLE I. Comparison of Bethe–stopping-power–theory parameters, Z_e, $L(0)$, and I, calculated with optical oscillator strengths, with similar calculations for Ar from Ref. 10. The experimental I values for Ar, Kr, and Xe are from Ref. 2.

	Z_e	$L(0)$	I (eV)
Ar (present)	17.81	45.38	174.0
Ar (calc.)	18.0	46.22	177.0
Ar (expt.)			194.0
Kr (present)	36.39	116.32	333.0
Kr (expt.)			376.0
Xe (present)	53.37	186.88	451.0
Xe (expt.)			497.0

III. EXTRACTION OF STOPPING-POWER PARAMETERS FROM THE EXPLICIT CALCULATIONS

Numerical stopping-power results calculated in the nonrelativistic PWBA contain neither relativistic effects nor effects proportional to Z_1^3 or Z_1^4. They do contain shell corrections. The standard nonrelativistic treatment of stopping power $[S_T = -(1/n)dE/dx = \sum S_T^{nl}]$ begins with

$$S_T = 4\pi a_0^2 \frac{M_e}{M_p} \frac{1}{E_p} E_H(\text{eV}) \times 2Z_e \left[\ln\left[\frac{4M_e}{M_p} \frac{E_p}{I} \right] - \sum_{n,l} C_{nl} \right] , \tag{5}$$

where a_0 is the Bohr radius, E_H is 13.6 eV, and C_{nl} is the inner-shell correction, which goes to zero as E_p goes to infinity. In numerical terms, and using Eqs. (2)–(4) on a subshell basis[5] we can write

$$Z_{nl} \ln I_{nl} + C_{nl} = Z_{nl} \ln \left[\frac{4M_e}{M_p} E_p \right] - 4.19\times 10^{+15} E_p S_T^{nl} \;. \tag{6}$$

If this analysis were sufficient to extract I_{nl} and C_{nl} results from the explicit PWBA calculations, the right-hand side of Eq. (6) would approach a constant as E_p approached infinity and the constant would be $Z_{nl}\ln I_{nl}$ as calculated using optical oscillator strengths. Here, as in Ref. 5, neither condition is found to apply. On the other hand, as in Ref. 5, if one uses

$$(Z_n \ln I_n)^* + C_{nl} = Z_n^* \ln \left[\frac{4M_e}{M_p} E_p \right] - 4.19\times 10^{+15} E_p(\text{MeV}) S_T^{nl} \tag{7}$$

and requires

$$\lim_{E_p\to\infty} 4.19\times 10^{+15} E_p(\text{MeV}) S_T^{nl} = Z_{nl}^*(\beta E_p) \;, \tag{8}$$

TABLE II. Comparison of Z_{nl} and Z_{nl}^* values for Ar, Kr, and Xe.

	Ar		Kr		Xe		
Subshell	Z_{nl}	Z_{nl}^*	Z_{nl}	Z_{nl}^*	Z_{nl}	Z_{nl}^*	$\frac{1}{2}(Z_{nl}+N_{nl})$
1s	1.45	1.83	1.25	1.93	1.22	1.69	1.61
2s	1.36	1.56	1.48	1.62	1.15	1.58	1.575
2p	6.91	6.35	4.95	5.57	3.17	4.67	4.59
3s	0.62	1.30	1.21	1.57	1.19	1.68	1.60
3p	7.47	6.68	4.13	5.24	4.79	5.39	5.40
3d			14.73	12.23	13.80	11.96	11.90
4s			0.47	1.20	0.94	1.53	1.47
4p			8.17	6.79	3.46	4.69	4.73
4d					15.49	12.81	12.75
5s					0.30	1.18	1.15
5p					7.86	6.93	6.93
Total	17.81	17.72	36.39	36.24	53.37	54.11	53.71

where β is a constant, then one obtains Z_{nl}^* from the asymptotic behavior of S_T^{nl}. Further, using Eq. (7), one can determine $(Z_{nl}\ln I_{nl})^*$, as C_{nl} goes to zero when $E_p \rightarrow \infty$. Then I, found from

$$\ln I = \sum_{n,l} (Z_{nl}\ln I_{nl})^* \Big/ \sum_{n,l} Z_{nl}^* , \quad (9)$$

is the Bethe parameter found from the explicit PWBA stopping-power calculations. Further, the subshell corrections are found from

$$C_{nl} = Z_{nl}^* \ln\left[\frac{4M_e}{M_p}E_p\right] - 4.19\times 10^{+15} E_p(\mathrm{MeV}) S_T^{nl} - (Z_{nl}\ln I_{nl})^* . \quad (10)$$

Bethe *et al.*[11] have shown that the coefficient of $\ln I_{nl}$ should be $\frac{1}{2}(N_{nl}+Z_{nl})$ in hydrogenic cases. In Table II, are listed the Z_{nl} values obtained from optical oscillator strengths, and the Z_{nl}^* values obtained from the explicit calculations for Ar, Kr, and Xe. For Xe, I list also the values of $\frac{1}{2}(Z_{nl}+N_{nl})$. These latter values are remarkably close to the Xe Z_{nl}^* values.

In Table III are listed the $L_{nl}(0)$ values obtained from optical oscillator strengths and $L_{nl}(0)^*$ obtained from the explicit calculations. In general (the Kr 2s subshell is an exception), as expected from the shift of an effective number of electrons in Z_{nl}^* compared to Z_{nl}, the $L_{nl}^*(0)$ values for the inner shells are larger than the $L_{nl}(0)$ values. For the outer shells one might expect $L_{nl}(0) > L_{nl}^*(0)$, but this expectation must be modified as the discrete vs continuum contributions are often quite different in evaluating $L_{nl}(0)$ and $L_{nl}(0)^*$.

Table III points out several interesting features. First, the I values obtained from the explicit calculations are larger than the I values inferred from experiment, by 9 eV

TABLE III. Comparison of $L_{nl}(0)$ and $L_{nl}(0)^*$ values for Ar, Kr, and Xe, and I and I/Z values.

	Ar		Kr		Xe	
Subshell	$L_{nl}(0)$	$L_{nl}(0)^*$	$L_{nl}(0)$	$L_{nl}(0)^*$	$L_{nl}(0)$	$L_{nl}(0)^*$
1s	8.72	9.19	9.35	13.37	10.14	12.38
2s	5.58	6.35	8.34	7.85	7.69	9.37
2p	24.01	23.56	26.42	28.58	20.11	28.82
3s	1.60	1.49	5.02	6.69	6.36	9.83
3p	5.47	7.28	16.31	19.10	24.03	25.07
3d			45.62	41.35	62.76	58.26
4s			1.21	1.09	3.70	6.17
4p			4.05	3.24	12.84	12.32
4d					38.30	34.52
5s					0.74	1.30
5p					0.21	3.00
Total	45.38	47.87	116.32	121.27	186.88	201.04
I (eV)	174.00	203.00	333.00	386.00	451.00	559.00
I/Z (eV)	9.67	11.27	9.25	10.72	8.35	10.35

TABLE IV. Inner-shell corrections for Ar.

E (MeV)	1s	2s	2p	3s	3p	Total
0.1		−2.04	−6.10	0.57	1.08	−6.49
0.2		−1.09	−2.20	0.78	1.50	−1.01
0.3		−0.64	−0.31	0.92	1.98	1.95
0.4		−0.39	0.75	0.92	1.63	2.91
0.5		−0.23	1.39	0.71	1.20	3.07
0.6		−0.13	1.81	0.55	0.92	3.15
0.7		−0.07	2.04	0.43	0.76	3.16
0.8		−0.02	2.20	0.33	0.64	3.15
1	0.07	0.06	2.32	0.25	0.09	2.79
2	1.22	0.25	2.14	0.01	0.04	3.66
3	1.78	0.34	2.07			4.19
4	2.09	0.46	2.08			4.63
5	2.29	0.58	2.20			5.07
6	2.41	0.70	2.06			5.17
7	2.49	0.77	1.55			4.81
8	2.54	0.72	1.13			4.39
10	2.60	0.55	0.55			3.70
20	2.62	0.25	0.05			2.92
30	2.59	0.16				2.75
40	2.38	0.11				2.49
50	1.80	0.07				1.87
60	1.20	0.04				1.24
70	0.71	0.0				0.71
80	0.41					0.41
100	0.14					0.14

TABLE V. Inner-shell corrections for Kr.

E (MeV)	1s	2s	2p	3s	3p	3d	4s	4p	Total
0.1				−2.37	−4.76	−8.05	0.19	2.82	−12.2
0.2				−1.42	−1.71	−1.20	0.44	2.29	−1.60
0.3				−0.98	−0.33	1.89	0.65	1.44	2.67
0.4				−0.72	0.38	3.51	0.53	0.87	4.57
0.5			−4.27	−0.58	0.81	4.41	0.41	0.76	1.54
0.6		−0.49	−3.31	−0.47	1.07	4.91	0.30	0.61	2.62
0.7		−0.26	−2.52	−0.39	1.29	5.21	0.19	0.59	4.11
0.8		−0.07	−1.85	−0.31	1.40	5.40	0.16	0.49	5.22
1		0.24	−0.78	−0.20	1.60	5.59	0.16	0.64	7.25
2		0.99	1.91	0.17	2.27	5.51	0.04	0.41	11.3
3		1.28	2.84	0.42	1.79	4.05		0.35	10.7
4		1.40	3.21	0.33	1.35	2.40		0.42	9.11
5		1.49	3.32	0.24	1.06	1.63		0.26	8.00
6		1.55	3.33	0.17	0.82	1.02		0.16	7.05
7	0.09	1.59	3.29	0.11	0.65	0.87		0.16	6.76
8	0.32	1.64	3.27	0.08	0.52	0.55		0.10	6.48
10	0.67	1.73	3.13	0.03	0.37	0.53			6.46
20	1.54	1.99	2.55	0.01	0.06	0.10			6.25
30	1.83	1.39	1.16						4.38
40	1.96	0.95	0.30						3.21
50	2.02	0.72	0.11						2.85
60	2.06	0.55							2.61
70	2.08	0.39							2.47
80	2.11	0.30							2.41
100	2.12	0.16							2.28
200	1.76	0.0							1.76
300	0.59								0.59
400	0.08								0.08

TABLE VI. Inner-shell corrections for Xe.

E (MeV)	1s	2s	2p	3s	3p	3d	4s	4p	4d	5s	5p	Total
0.1				−5.17	−10.13	−25.11	−2.12	−0.12	−2.32	−0.45	1.37	−44.05
0.2				−4.01	−6.42	−16.90	−1.36	1.89	2.20	−0.15	2.16	−22.59
0.3				−3.34	−4.31	−12.19	−1.00	2.68	3.78	0.13	2.02	−12.23
0.4				−2.88	−2.87	−8.95	−0.80	3.13	4.50	0.34	1.64	−5.89
0.5				−2.54	−1.81	−6.53	−0.64	3.43	4.90	0.44	1.37	−1.38
0.6				−2.28	−0.99	−4.63	−0.53	3.65	5.22	0.38	1.18	2.00
0.7				−2.08	−0.35	−3.10	−0.44	3.87	4.91	0.32	1.05	4.18
0.8				−1.92	0.16	−1.85	−0.36	4.05	4.42	0.26	0.96	5.72
1		−1.38		−1.67	0.92	0.07	−0.22	4.33	3.45	0.19	0.83	6.52
2		−0.33		−1.16	2.46	4.17	0.26	4.69	1.51	0.07	0.52	12.19
3		0.20	−0.47	−0.95	2.96	5.12	0.18	3.70	0.72	0.04	0.44	11.94
4		0.53	0.52	−0.81	3.23	5.25	0.09	3.00	0.34	0.02	0.38	12.55
5		0.74	1.15	−0.70	3.48	5.17	0.05	2.56	0.43		0.16	13.04
6		0.88	1.57	−0.59	3.67	5.05	0.03	2.20	0.17		0.34	13.32
7		0.99	1.85	−0.50	3.83	4.99	0.02	1.88	0.30		0.48	13.84
8		1.07	2.02	−0.42	4.01	4.93	0.01	1.64	0.17		0.32	13.75
10	0.067	1.17	2.19	−0.29	4.28	4.05		1.31	0.09		0.36	13.23
20	1.12	1.51	2.06	0.17	2.57	0.99		0.66			0.22	9.30
30	1.63	1.77	1.80	0.31	1.48	0.14		0.55			0.05	7.73
40	1.91	1.94	1.71	0.21	0.68			0.48				6.93
50	2.08	2.06	1.82	0.14	0.29			0.31				6.70
60	2.18	2.13	1.54	0.10	0.08			0.28				6.31
70	2.25	2.00	1.18	0.09				0.34				5.86
80	2.30	1.84	0.91	0.07				0.11				5.23
100	2.37	1.31	0.57					0.04				4.29
200	2.57	0.38	0.16									3.11
300	2.56	0.06	0.12									2.74
400	2.42											2.42
500	1.84											1.84
600	1.28											1.28
700	0.789											0.79
800	0.458											0.46
1000	0.165											0.17

in Ar and 10 eV in Kr, but by 62 eV in Xe. Second, the I values obtained from the explicit calculations are closer to the experimental values than the I values obtained from the optical oscillator strengths, except for Xe. Considering that the calculated stopping power for Xe agrees as well with the measurement of Ref. 9 at 4.4 MeV, as do the calculations for Ar and Kr, suggests that the I value of Ref. 2 for Xe may be in error. The measurements in Ref. 2 (below 1 MeV) agree well with the measurements of Ref. 6 and these measurements[2] were used to determine a Xe I value.

One possible reason for the discrepancy between the calculated and experimental I value may lie in the inner-shell correction used in the analysis of experimental data in Ref. 2, i.e., the correction of Bonderup[12] determined from a modified free-electron–gas model. I discuss inner-shell corrections in the next section.

The extraction of subshell stopping-power parameters from the explicit calculations requires the graphical determination of Z^*_{nl}. In Fig. 2, I show $4.19\times10^{+15}\times E_p(\mathrm{MeV})S^{nl}_T$ as a function of $\ln E_p$ as circles for the Ar 1s shell, and as circles, squares, and triangles for the Kr 1s, 2s, and 2p subshells. The solid lines are the asymptotic expressions

$$4.19\times10^{+15}E_pS^{nl}_T=Z^*_{nl}\ln E_p+Z^*_{nl}\ln\beta \ .$$

Figure 2 indeed indicates that the nonrelativistic calculations do approach the appropriate asymptotic form, but

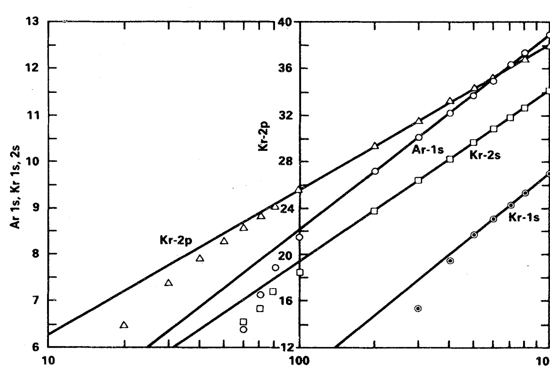

FIG. 2. Explicit values of $4.19\times10^{+15}E_p(\mathrm{MeV})S_{nl}$, used to determine Z^*_{nl} for the Ar 1s shell, and the Kr 1s, 2s, and 2p subshells.

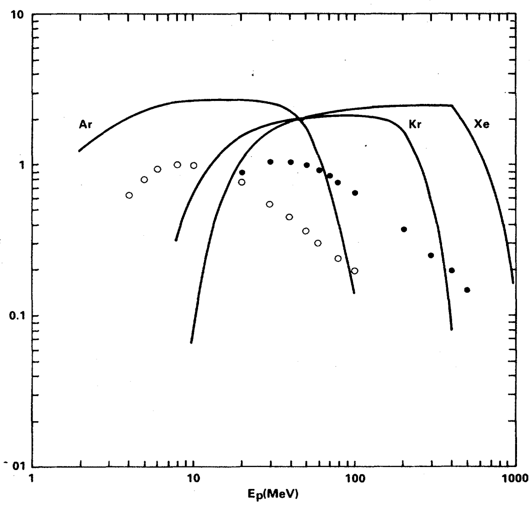

FIG. 3. Comparison of my C_K values (solid lines) with the hydrogenic values of Ref. 13 for Ar (open circles) and Kr (solid circles).

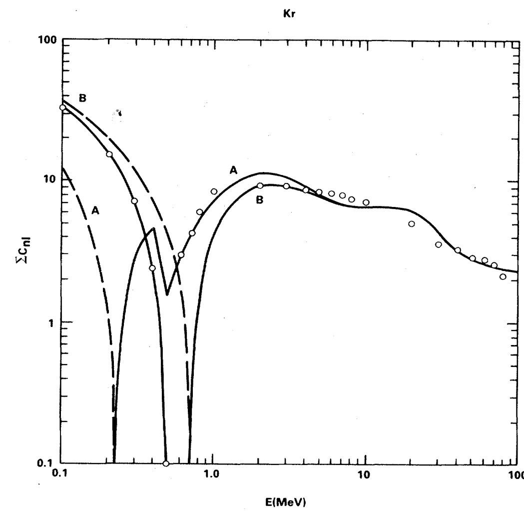

FIG. 5. Comparison of my total inner-shell corrections ($\sum_{n,l} C_{nl}$) with the statistical-model results (open circles) of Ref. 12 for Kr. The dashed lines are negative values.

for these four subshells, only when the explicit calculations are extended to 1 GeV.

IV. THE INNER-SHELL CORRECTIONS

In Tables IV—VI are listed the inner-shell corrections found from Eq. (10) and the explicit calculations. When the explicitly calculated subshell stopping power is negligible (low E_p), the entry is left blank. In a treatment[13] of stopping power based on subshell sums there is neither a contribution to stopping power nor a correction for such energies. This situation is referred to as case A. Using the global (all occupied subshells included via a single I value) treatment of the Bethe formula, at these low energies the correction is given by

$$Z_{nl}^{*}\ln(4M_eE_p/M_p)-(Z_{nl}^{*}\ln I_{nl})^{*} . \tag{11}$$

When these terms are included one has case B. In Tables IV—VI are listed the subshell corrections for Ar, Kr, and Xe. In Fig. 3 the K-shell corrections are plotted and compared with the hydrogenic calculations of Walske.[14] As was the case for Al,[5] the K-shell corrections are a factor of 2—2.5 larger than Walske's values. In addition, my corrections show a broad plateau region at the maximum whereas Walske's show only a peak at the maximum. A study of the K-shell correction for Al ions as a function of the degree of ionization for comparison with the hydrogenic results will be published.[15]

In Figs. 4—6, I show the total inner-shell correction [case A from Tables IV—VI, and case B including Eq. (11)]. At low energy the corrections are negative and I

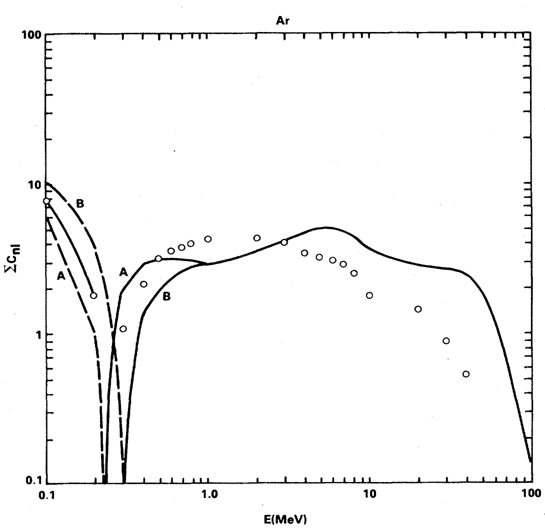

FIG. 4. Comparison of my total inner-shell corrections ($\sum_{n,l} C_{nl}$) with the statistical-model results (open circles) of Ref. 12 for Ar. The dashed lines are negative values.

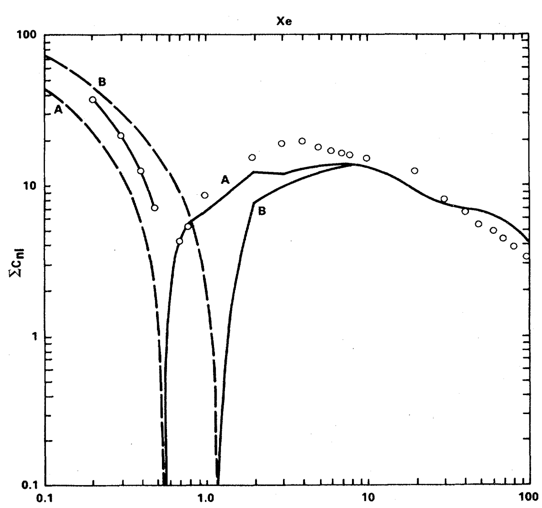

FIG. 6. Comparison of my total inner-shell corrections ($\sum_{n,l} C_{nl}$) with the statistical-model results (open circles) of Ref. 12 for Xe. The dashed lines are negative values.

show these as dashed curves. The open points are from Bonderup's[12] calculations with my interpolation (Bonderup presents results for Al, Cu, and Au).

For Kr the two sets of calculations are in excellent agreement, while for Ar and Xe the agreement is only qualitative. Note also that above 1 MeV Bonderup's correction agrees more closely with the case A results.

The inner-shell corrections enter the determination of the mean excitation energy via

$$\ln I_m = \ln I + (1/Z_e)\sum_{n,l} C_{nl} , \quad (12)$$

where I_m is the measured I value in the absence of shell corrections. Figures 4—6 allow one to estimate the variation in inferred I values in Ref. 2 due to the difference in $\sum_{n,l} C_{nl}$. The data in Ref. 2 are in the 0.1—1 MeV regime. For Ar in this range the case A $\sum_{n,l} C_{nl}$ differs from Bonderup's by the order of one unit, changing $\ln I$ by $\frac{1}{18}$. This changes the inferred I value by ± 10 eV, i.e., $I(\mathrm{Ar}) = 194 \pm 10$ eV. For Ar in the 0.4—1-MeV regime, the case-B results are almost exactly one unit lower than Bonderup's correction. This difference would change the inferred I value from 194 to 204 eV, in excellent agreement with the value obtained from the Z^*_{nl} analysis in Table III (i.e., $I = 203$ eV).

For Kr the case A results agree with Bonderup's from 0.6 to 1 MeV. The case B results are generally four units smaller. This difference would change the inferred Kr I value from 376 to 420 eV. This is somewhat larger than the value obtained from analysis of the explicit calculations ($I = 386$ eV).

For Xe between 0.3 and 1 MeV, the case-B results are smaller than Bonderup's by 10 units. This will change the I value from 497 to 598 eV. The I value obtained from the analysis of the explicit calculations was $I = 559$ eV.

These variations in I values arising from variations in total inner-shell corrections are not small for atoms of intermediate and high Z. The comparison of two sets of inner-shell corrections in Figs. 4—6 indicate that there are energy regimes where the difference in corrections are small or zero. To minimize the error in an I value inferred from experiment, measurements should be made in these energy regimes.

V. Z^3 AND Z^4 CORRECTIONS

In an earlier publication,[16] the accuracy of the PWBA in calculating the neutral-atom stopping power above 0.1 MeV was estimated at 15%. The estimate was based on the difference between the calculation (solid curve in Fig. 1) and measurements in Xe. However, the measurements shown in Fig. 1 do include Z^3 and Z^4 effects. Andersen *et al.*[17] have empirically determined Z^3 and Z^4 corrections, and present them in the form

$$S_T = 4\pi a_0^2 \frac{M_e Z_e}{M_p E_p} Z_1^2 (L_0 + Z_1 L_1 + Z_1^2 L_2) , \quad (13a)$$

where for protons $Z_1 = 1$. Using

$$L_0 = 4.19\times 10^{15} E_p(\mathrm{MeV}) S_T^c / Z_e , \quad (13b)$$

where S_T^c is the stopping power without Z_1^3 and Z_1^4 corrections, Andersen *et al.*[17] find

$$L_1 = (L_0 / Z_e^{1/2})[(2.68/U)(1-0.132\ln U)] , \quad (13c)$$

where

$$U = M_e E_p(\mathrm{Ry}) / M_p (Z_2)^{2/3} \quad (13d)$$

and

$$L_2 = -1.6 M_p / M_e E_p(\mathrm{Ry}) , \quad (13e)$$

providing

$$E_p(\mathrm{Ry}) > 2.25 (Z_e)^{2/3} M_p / M_e . \quad (13f)$$

Inclusion of these Z^3 and Z^4 corrections results in the dashed curves in Fig. 1. For Ar above 0.3 MeV, the data and the dashed curve agree to better than 5%. For Xe, the dashed curve is in excellent agreement with the measurement of Reynolds *et al.*[6] at 0.6 MeV (the low-energy limit of the L_1 value of Anderson *et al.*[17]), suggesting that the 15% accuracy estimate for the PWBA calculations, based on Xe, is a significant overestimate. However, inclusion of the Z^3 and Z^4 correction destroys the excellent agreement between the calculations and experiment for Kr. The maximum difference (at 0.4 MeV) between calculation and experiment for Kr is now 15%, leaving the error estimate for PWBA stopping-power calculations unchanged.

VI. CONCLUSIONS

With the procedure developed for extracting Bethe stopping-power theory parameters from explicit PWBA calculations, I find I values within 10 eV of the experimentally inferred I values for Ar and Kr, but 60 eV higher than the value for Xe. The traditional procedure for determining atomic I values by summing over optical oscillator strengths produces I values that are significantly lower (17—20 eV in Ar, 43 eV in Kr, and 46 eV in Xe) than the experimentally inferred values. Inner-shell corrections are obtained from the PWBA calculations. For the Ar and Kr K-shells, my corrections are roughly a factor of 2 larger than the hydrogenic results of Walske.[14] Bonderup[12] has calculated total inner-shell corrections using a statistical model. My results are in qualitative agreement with his for Ar, Kr, and Xe. However, the quantitative differences between the two sets of inner-shell corrections can change the experimentally inferred I values significantly, i.e., by 10 eV in Ar, 46 eV in Kr, and 100 eV in Xe, in experimental data in the 0.1—1-MeV regime is used. I suggest that for the noble gases there are energy regimes where the difference between the two sets of inner-shell corrections is small, and these energy regimes can provide I values where the error arising from innershell corrections is minimized.

Comparison of explicit PWBA calculations of stopping power with experiment led to an error estimate of 15% for the PWBA calculations based on the comparison for Xe. Correction of the calculations for Z^3 and Z^4 effects (not present in PWBA calculations) leads to differences much less than 15% for Ar and Xe, but introduces a 15% difference for Kr—not changing the error estimate for PWBA stopping-power calculations.

ACKNOWLEDGMENTS

This work was supported by the U. S. Department of Energy. I want to thank L. C. Pitchford for doing the optical—oscillator-strength summations and J. M. Peek for valuable comments.

[1]H. A. Bethe, Ann. Phys. (Leipzig) 5, 325 (1930); Z. Phys. 76, 293 (1932).
[2]R. Besenbacher, H. H. Andersen, P. Hvelplund, and H. Knudsen, K. Dan. Vidensk. Selskab. Mat. Fys. Medd. 40, 3 (1979).
[3]E. J. McGuire, L. C. Pitchford, and J. M. Peek, Phys. Rev. A 26, 1318 (1982).
[4]E. J. McGuire, Phys. Rev. A 26, 1871 (1982).
[5]E. J. McGuire, Phys. Rev. A 28, 49 (1983).
[6]H. K. Reynolds, D. N. F. Dunbar, W. A. Wenzel, and W. Whaling, Phys. Rev. 92, 742 (1953).
[7]A. B. Chilton, J. N. Cooper, and J. C. Harris, Phys. Rev. 93, 413 (1954).
[8]J. B. Swint, R. M. Prior, and J. J. Ramirez, Nucl. Instrum. Methods 80, 134 (1970).
[9]J. E. Brolley, Jr. and F. L. Ribe, Phys. Rev. 98, 1115 (1955).
[10]J. L. Dehmer, M. Inokuti, and R. P. Saxon, Phys. Rev. A 12, 102 (1975).
[11]H. A. Bethe, L. M. Brown, and M. C. Walske, Phys. Rev. 79, 413 (1950).
[12]E. Bonderup, K. Dan. Vidensk. Selskab. Mat. Fys. Medd. 35, 1 (1967).
[13]E. J. McGuire (unpublished).
[14]M. C. Walske, Phys. Rev. 88, 1283 (1952).
[15]E. J. McGuire, Phys. Rev. A 28, 57 (1983).
[16]E. J. McGuire, Phys. Rev. A 26, 1858 (1982).
[17]H. H. Andersen, J. F. Bak, H. Knudson, and B. R. Nielson, Phys. Rev. A 16, 1929 (1977).